https://doi.org/10.5194/se-2020-135
Preprint. Discussion started: 2 September 2020

Solid Earth Discussions

Structural features derived from a Multiscale Analysis and 2.75D Modelling of Aeromagnetic Data over the Pitoa-Figuil Area (Northern Cameroon)

Voltaire Souga Kassia[a]; Theophile Ndougsa Mbarga[a,b*]; Arsène Meying[c]; Jean Daniel Ngoh[a]; Steve Ngoa Embeng [a]

[a]Postgraduate School of Science, Technology and Geosciences, University of Yaoundé I, Yaoundé, Cameroon
[b]Department of Physics, Advanced Teacher's Training College, University of Yaoundé I, P.O. Box 47, Yaoundé, Cameroon
[c]School of Geology and Mining Engineering, University of Ngaoundéré, P.O. Box 115, Meiganga, Cameroon

Correspondence should be addressed to Ndougsa Mbarga Theophile; *tndougsa@yahoo.fr

ABSTRACT:
In the Pitoa-Figuil area (Northern Cameroon), an interpretation of aeromagnetic data was conducted. The aim of this investigation was first to emphasize lineaments hidden under geological formations and secondly to propose two 2.75D models of the subsurface structures. Different magnetic data processing techniques were used, notably horizontal gradient magnitude, analytic signal, and Euler deconvolution. These techniques in combination with the 2.75D modelling to the aeromagnetic anomaly reduced to the equator permit to understand the stratification of the deep and near surface structures, which are sources of the observed anomalies. We managed to put in evidence and characterize 18 faults and some intrusive bodies. According to Euler's solutions, anomaly sources go up to a depth of 5.3 km.

Keywords: Horizontal gradient magnitude, Euler deconvolution, 2.75D modelling, Fault, Intrusive body.

1. Introduction

Investigating depths through geomagnetic field properties is the basis of the magnetic method, the one we used for this research.

This study is focused on a well-defined area in the northern Cameroon. Several studies (Ntsama et al., 2014; Kamguia et al., 2005) reveal the presence of many Cretaceous sedimentary basins. At the beginning of the Cretaceous age, the basement of the northern Cameroon region was affected by a tectonic event due to the Benue trough set up, which generated faults that promote volcanic activities (Ntsama et al., 2014). The resulting basaltic lava flows and the accumulated alluvial deposits in Mayos buried these faults.

The aim of this research paper is firstly to highlight magnetic anomalies and correlate them with the tectonic and geological events given by existing literature in order to locate and identify buried faults. Secondly, this article tries to make its contribution to the knowledge of the

https://doi.org/10.5194/se-2020-135
Preprint. Discussion started: 2 September 2020

Solid Earth Discussions

stratification of the Pitoa-Figuil subsurface. To achieve these purposes, some techniques such as Analytic signal, Euler deconvolution and 2.75D modelling were applied.

2. Geological and tectonic setting

Fragment of the Pan-African Belt in the northern part of Cameroon, between the longitudes 13°30' - 14°15' E and latitudes 09°15' - 09°45' N, the studied area covers several cities among which the most historical are Pitoa and Figuil. The basement complex consists of migmatite and ectinitic rocks from the Precambrian. The sedimentary basins in and around the studied area were set up in the Cretaceous by the NE-SW Benue trough which is one of the direct consequences of the establishment of the gigantic moat covered by the Atlantic Ocean (Ntsama et al., 2014).

The various geological formations and structures of the said zone are identified on Fig. 1 and can be grouped as follows (Toteu et al., 2004):

- Superficial formations (Q^3) from the Quaternary age;
- Cretaceous sedimentary formations (Ci, Cm);
- Precambrian formations namely ectinites (ξ^1, ξ^2, ζ^1, ζ^2), migmatites (M^1, M^2), ancient eruptive rocks (γ^1, γ^2) and micaceous quartzites.

Effusive rocks are also present, notably the rhyolites and rhyolitic tuffs of the Tertiary, as well as the undifferentiated monchiquite basalts of the Benue valley which are from the Cretaceous age.

The Mayo Oulo-Léré basin (Ci), which is the eastward branch of the Benue trough, extends for about 50 km (length) with a width value for about 9 km (Ntsama et al., 2014).

Two NE-SW tectonic lines mark the studied area: one at the west of Boïli and the other at the West of Golombe. Most dips are vertical. The migmatite gneisses formation at the geological map centre is intruded by a NE-SW veins of quartz. Ntsama et al. (2014) revealed the presence of faults buried under geological formations. Most orthogneisses and migmatites come from the transformation of granitoids due to the Panafrican deformation D2 (Daouda, 2014).

On the structural aspect, the northern Cameroon domain is marked by two deformation phases (Toteu et al., 2004):

- The first phase is characterised by a foliation with variable dip and direction;
- The second one is characterised by tight and straight folds associated to a vertical axial plane foliation.

https://doi.org/10.5194/se-2020-135
Preprint. Discussion started: 2 September 2020

Solid Earth
Discussions

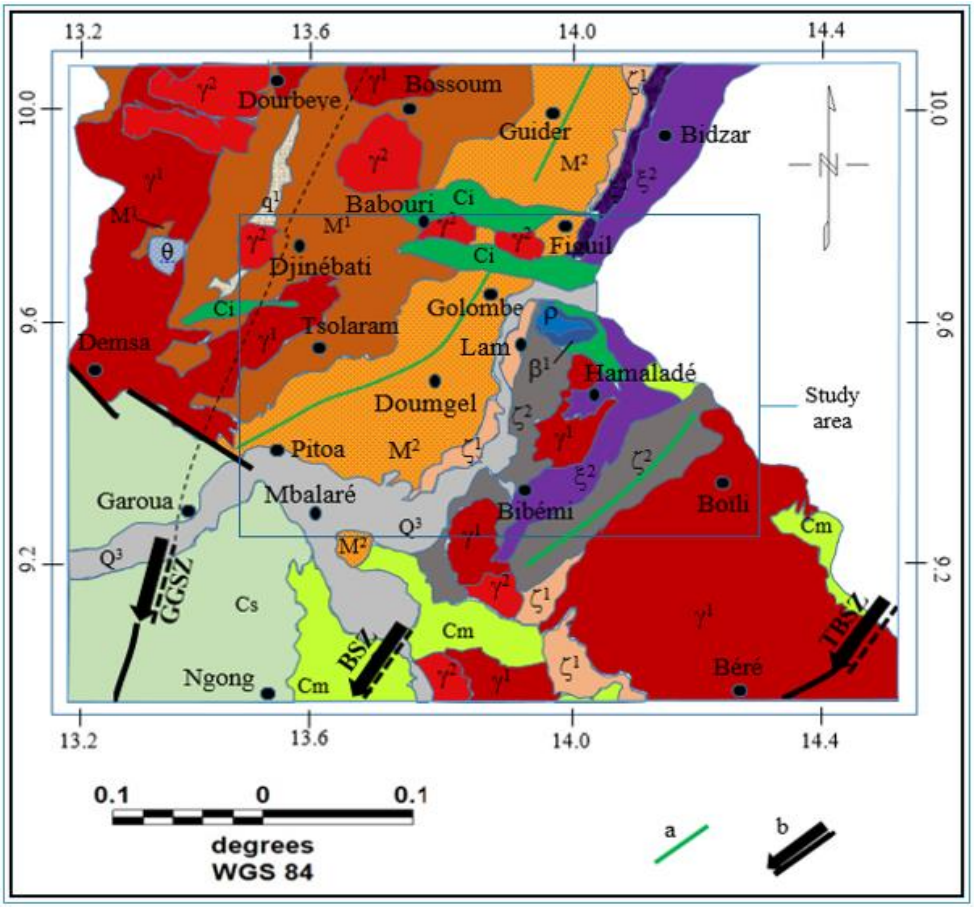

Figure 1: Geological map of the studied area (redrawn from Ngako et al., 2008; Elangwe, 1979 ; this map is available at the public domain): (γ^1) Anatexia granites and granodiorites; (γ^2) Monzonitic late syntectonic granites; (M^1) Biotite anatexite; (M^2) Migmatitic gneisses; (ζ^1) Lower gneisses: biotite, amphibole and pyroxene cross-cut by intrusive quartz; (ζ^2) Upper gneisses: grenatiferous with two micas; (ξ^1) Lower micaschists of the Poli Group; (ξ^2) Upper micaschists with chlorites of the Poli Group; (q^1) Micaceous quartzites; (β^1) Undifferentiated monchiquite basalts of the Bénoué valley; (Q^3) Alluviums and lacustrine clays; (θ) Gabbros; (ρ) Ryolites and ryolitic tuffs; (Ci) Amakassou and Kontcha sandstone conglomerate and schisto-clays; (Cm) Bénoué and Kontcha sandstone; (Cs) Garoua sandstone; (a) Tectonic lines; (b) Shear zones: Godé-Gormaya shear zone (GGSZ), Tchollіré-Banyo shear zone (TBSZ).

3. Materials and methods

In 1970, aeromagnetic data were collected by the company SURVAIR (Canada) for the Federal Republic of Cameroon. After correction of data resulting from this survey, Paterson et al. (1976), established magnetic maps and included them in their final report. These magnetic maps are the starting point and the key component of this study. We used MapInfo v11.0 to digitize them. Then, through the Oasis montaj software v8.4, we subtracted the International Geomagnetic Reference Field (IGRF) from the measured field to obtain the total magnetic intensity (TMI).

https://doi.org/10.5194/se-2020-135
Preprint. Discussion started: 2 September 2020

In the present paper, data filtering techniques were implemented using the Oasis montaj software v8.4.

3.1. Reduction to Magnetic Equator

For further data interpretation, the reduction to magnetic equator (RTE) technique is much more used in the equatorial zones to centre the magnetic anomalies in line with their sources.

The RTE is calculated following Eq. (1) (Leu, 1981):

$$R(\vartheta) = -\frac{\left[A(I)-i\cos(I).\cos(D-\theta)^2\right]\times\cos^2(D-\theta)}{\left[A^2(Ia)+\varphi^2(Ia,D)\right]\times\left[A^2(I)+\varphi^2(I,D)\right]} \qquad (1)$$

Where:

I is the geomagnetic inclination;

D is the geomagnetic declination;

$A(I)=sin(I)$ is the RTE amplitude;

$\Phi(I,D)=cos(I).cos(D-\vartheta)$ is the RTE phase;

Ia is the inclination for RTE amplitude correction.

The RTE technique was applied to the TMI anomalies where -2.588° were used as the inclination value and -4.132° as declination at 1st January 1970 which is the date corresponding to the period of which data were collected.

3.2. Horizontal Gradient Magnitude

The horizontal gradient magnitude (HGM) is a filtering technique usually used for potential fields. It makes it possible to highlight lithological contacts of bodies in basement.

The HGM is given by Eq. (2) (Cordell and Grauch, 1982):

$$HGM\ (x,y) = \sqrt{\left(\frac{\partial M(x,y)}{\partial x}\right)^2+\left(\frac{\partial M(x,y)}{\partial y}\right)^2} \qquad (2)$$

Where the magnetic field is $M\ (x, y)$.

Vertical body edges are generally located through the maxima of HGM (Awoyemi et al., 2016).

3.3. Analytic Signal Method

The strong magnetizations of the analytic signal (AS) make it possible to highlight limit contacts of geological formations. The AS amplitude of magnetic anomaly is defined by Eq. (3) (Roest et al., 1992):

$$|AS(x,y)| = \sqrt{\left(\frac{\partial M(x,y)}{\partial x}\right)^2+\left(\frac{\partial M(x,y)}{\partial y}\right)^2+\left(\frac{\partial M(x,y)}{\partial z}\right)^2} \qquad (3)$$

The fact that the AS is a function always positive and therefore, does not require to know the direction of the magnetized body, is a major advantage of this technique compared to the others (Jeng et al., 2003).

3.4. Euler Deconvolution

Applied to aeromagnetic data, it is a technique which permits to locate sources of observed anomalies and determine their depths. This technique is based on an important parameter that

https://doi.org/10.5194/se-2020-135
Preprint. Discussion started: 2 September 2020

accounts for the degree of homogeneity of the mathematical equation that comes into play, this parameter is named "structural index" (Durrheim, 1998). The structural index (SI) characterizes the geological type of the source (dyke, sill, pipe, cylinder, and sphere) according to its value which varies between 0 and 3 for the case of magnetic data.

The Euler's homogeneity equation in this case is the Eq. (4) below (Whitehead and Musselman, 2005):

$$(x-x_0)\left(\frac{\partial T}{\partial x}\right)+(y-y_0)\left(\frac{\partial T}{\partial y}\right)+(z-z_0)\left(\frac{\partial T}{\partial z}\right) = N(M-T) \qquad (4)$$

Where:

(T is the total magnetic field produces at *(x, y, z) by* the magnetic source at (x_0, y_0, z_0);

M is the regional value of T;

N is the structural index (SI).

With four unknown parameters (x, y, z, M), solving the Euler's equation requires to consider a square window on the grids of gradients and field. However, this window must be sized to exclude unwanted anomalies while containing all significant solutions (Durrheim, 1998).

3.5. 2.75D modelling

When a source of anomalies presents a preferred extension in a given direction, profiles are interpreted perpendicularly to the main extension. The 2.75D model represents geological blocks as polygonal prisms either finite or infinite elongated following a strike direction named Y with horizontal axes (X). The plane of the profile and the Y direction need not to be perpendiculars (Rasmussen and Pedersen, 1979).

According to Skalbeck et al. (2005), the 2.75D modelling is a potential field modelling technique based on asymmetric strike length (Y) about the profile (X). The 2.75D modelling techniques are suitable for geological modelling, as potential field profiles may not cross a structure through its centre.

To build our magnetic models, we used the analyses of Talwani and Heirtzler (1964) and Rasmussen and Pedersen (1979). These models were obtained through GM-SYS™ which is an extension of Geosoft package software v8.4.

4. Results

4.1. RTE map

The map (Fig. 2) presents an irregular distribution of anomalies. The values in nanotesla (nT) of these anomalies range from -660.3 to 286.4 with various forms. It is thus possible to distinguish positive magnetic anomalies (dark pink and red colour) which are in great proportion on this map and a minority of negative magnetic anomalies (light and dark blue colour) which lodge the NE-SW axis.

The Lam area is marked by an elliptical bipolar anomaly with an E-W direction over a length of about 15.5 km. This anomaly has an intensity of -600 nT for the negative pole and 200 nT for the positive pole which is more developed than the negative one. The positive pole at this point correlates well with the geological map (Fig. 1), which indicates the presence of monchiquite basalts

https://doi.org/10.5194/se-2020-135
Preprint. Discussion started: 2 September 2020

Solid Earth Discussions
Open Access
EGU

of the Benue valley and rhyolitic tuffs which are rocks with a strong magnetic response. In short, these are anomalies that materialize the signature of a geological structure buried under the covers. The negative lobe suggests the presence of geological formations with low susceptibilities such as sandstone and shale clays as indicated on the geological map.

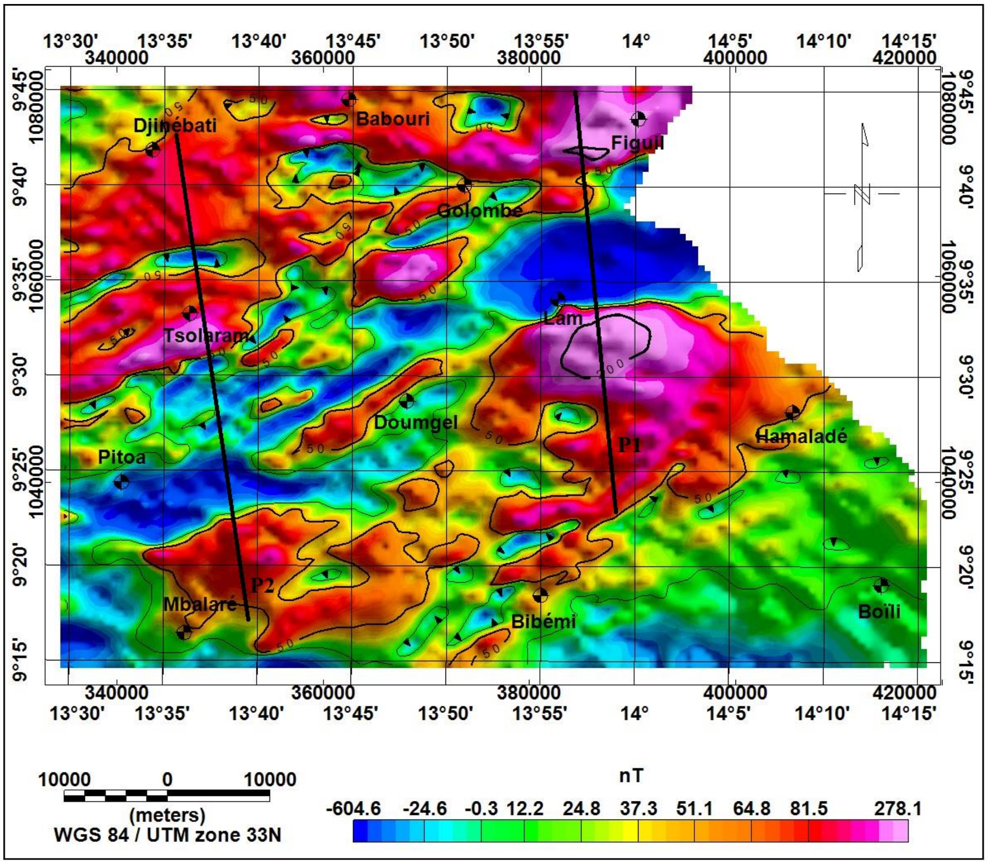

Figure 2: Color shaded reduction to equator (RTE) map.

The same observation is made in south of Pitoa where this time we have -400 nT for the negative pole and about 75 nT for the positive one with a mainly ENE-WSW direction.

In the western Doumgel, between the two previous bipolar anomalies, there is a group of small positive (70 nT) and negative (-500 nT) linear anomalies with ENE-WSW direction. The forms and directions of these anomalies and those of the southern Pitoa allow us to believe that they would be the outcome of the same tectonic event.

From the magnetic point of view, the subsurface in Northern Cameroon is perturbed by several anomalies with different wavelengths, most of them are related to the Precambrian basement formations. Some anomalies reflect sedimentary deposits. Bipolar anomalies could be interpreted as very deep geological structures hidden by extensive formations (Feumoe et al., 2012).

https://doi.org/10.5194/se-2020-135
Preprint. Discussion started: 2 September 2020

4.2. HGM map

The horizontal gradient magnitude technique is a great way to locate geological contacts in the basement and faults by determining their directions (Khattach et al., 2006). To better distinguish deeper geological structures, the HGM method is applied to the 2 km upward continued RTE map and the result is given by Fig. 3.

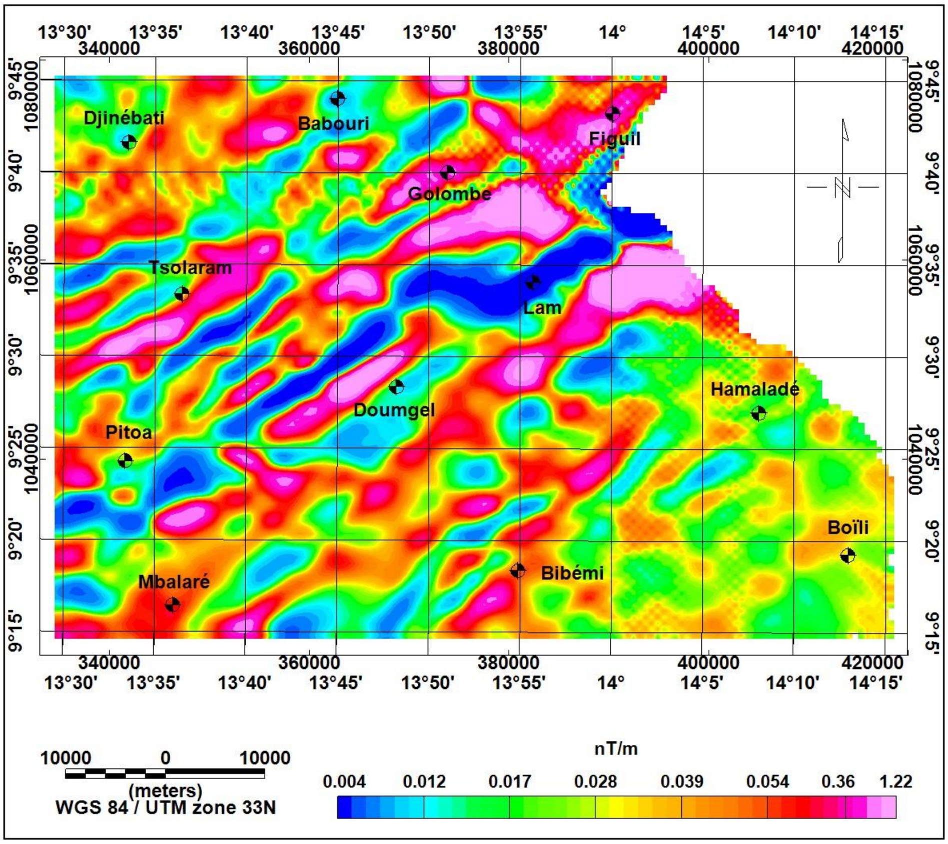

Figure 3: Horizontal Gradient Magnitude (HGM) map

There is a wide variety of anomalies, most of them are linear with different lengths and their amplitudes fluctuate between 0.004 and 1.22 nT/m.

The corresponding structures are mainly oriented in the NE-SW direction. Some elliptical and unformed anomalies around Figuil and at the northern Tsolaram are plainly observable. Outcrops or intrusive bodies can explain the high level of the amplitude gradients which characterize them. Many linear and curved bipolar magnetic anomalies are observed along the Pitoa-Figuil axis. Viewed their form, some of these anomalies are certainly magnetic responses of dykes or faults.

For automatic location of the HGM maxima, we adopted the Blakely and Simpson (1986) method. The resulting map (Fig. 5) shows that local maxima (green peaks) form narrow wrinkles above abrupt susceptibility fluctuations.

https://doi.org/10.5194/se-2020-135
Preprint. Discussion started: 2 September 2020

Solid Earth Discussions

On the centre of the map, more precisely in the area covered by the migmatite gneisses, the configuration of the NE-SW maxima suggests the presence of structural deformation at the regional scale in the basement stratums. This correlates well with the linear anomalies of the RTE map and are interpreted as being the direct consequences of the settlement of the Benue tectonic trough due to the opening of the Atlantic.

4.3. AS map

The AS method is applied to the 2 km upward continued RTE map and the result is given by Fig. 4. The high magnetic signals of the AS map correlate well with the magnetic response of migmatite rocks found in the Lam area and around the Figuil-Pitoa axis with a NE-SW trend. Geological contacts represented by harsh signal contrasts are emphasized; among them, appears the biotite anatexite - migmatite gneisses contact (white outline).

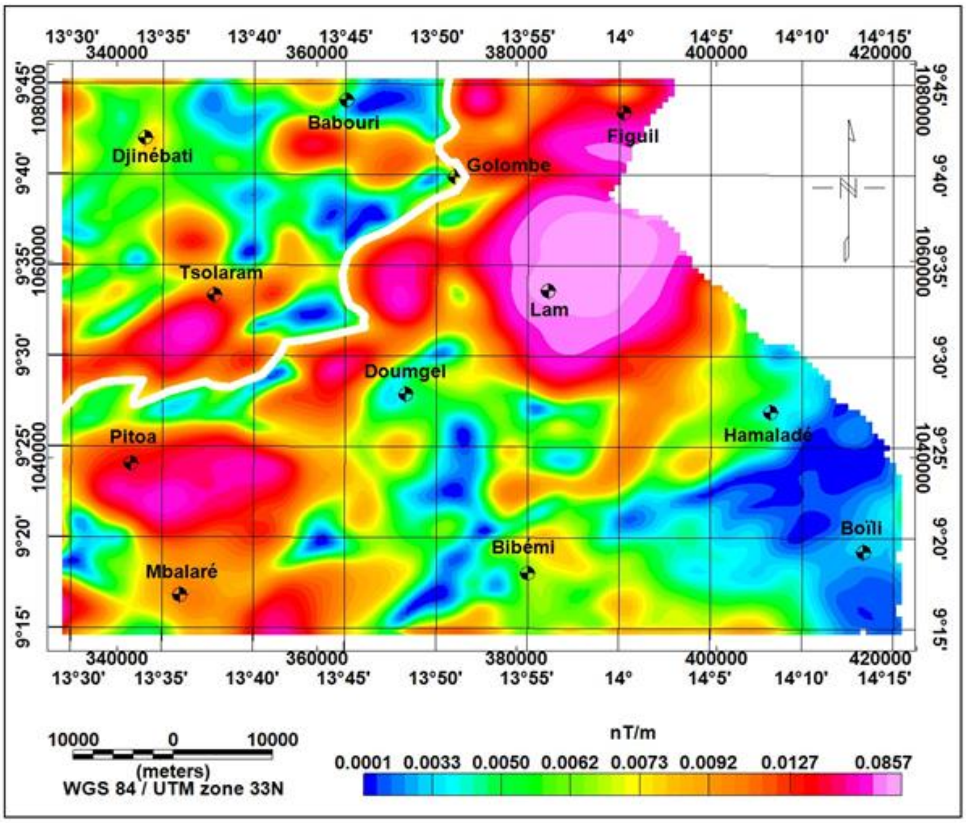

Figure 4: Analytic signal (AS) map

AS and HGM maxima were generated, pooled, and superimposed in a single map as shown on Fig. 5. Peaks are quasi-parallel this is the proof that the geological structures of our study region admit dips linked to dextral and senestral deformations which affected it (Ngako et al., 2008). The

https://doi.org/10.5194/se-2020-135
Preprint. Discussion started: 2 September 2020

Solid Earth Discussions
Open Access
EGU

maxima of the HGM are more abundant than those of the AS. According to Cordell and Grauch (1982), areas where the AS maxima are isolated, indicate the much deeper structures (southern Pitoa, Doumgel and Lam area).

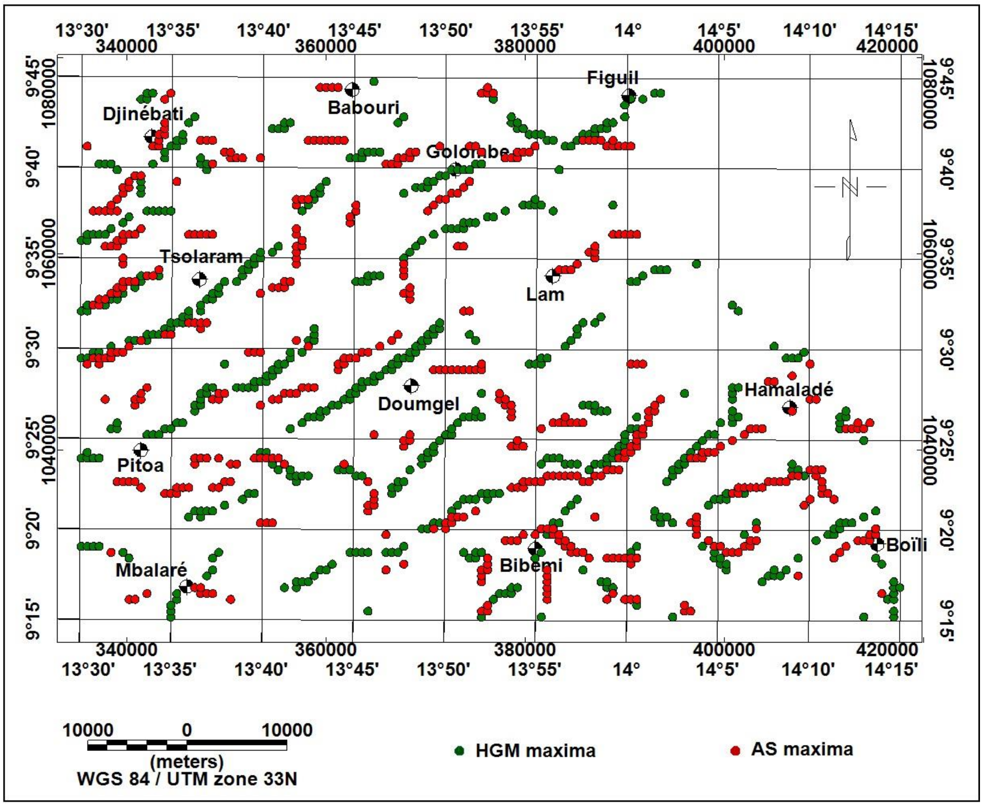

Figure 5: HGM (in green) and AS (in red) peaks map.

4.4. Euler's solutions map

The 2 km upward continued RTE map is the map on which was applied the Euler deconvolution method, to determine depths of anomaly sources by setting the flying height of plane observation at 235 m, the tolerance at 15% and the structural index at 1. Given the importance of the wavelength of anomalies and the value of the grid cell, we have chosen a Nyquist window size of 15 km × 15 km. The result is given by Fig. 6 below.

On the Euler's solutions map above, several structures with depth varying from 1400 to 5300 m are highlighted. We can clearly distinguish deep faults and intrusive bodies which are characterized by the non-linear or the stacking of Euler's solutions (Keating and Pilkington, 2004; Ndougsa et al., 2012). This is observed in the Lam area and southern Pitoa. Some of these intrusive bodies are located around the contact zone between the biotite anatexite and the migmatite gneisses stratums at a depth of about 4000 m. From this same interpretation, intrusive bodies at

https://doi.org/10.5194/se-2020-135
Preprint. Discussion started: 2 September 2020

Solid Earth
Discussions
Open Access
EGU

almost the same depth, are also perceived nearby the contact zone between upper gneisses and upper mica schists formations in the Eastern Bibémi.

As for rectilinear and continuous alignments of Euler's solutions found in the northern and western areas, they would be the magnetic signatures of normal faults hidden under geological formations.

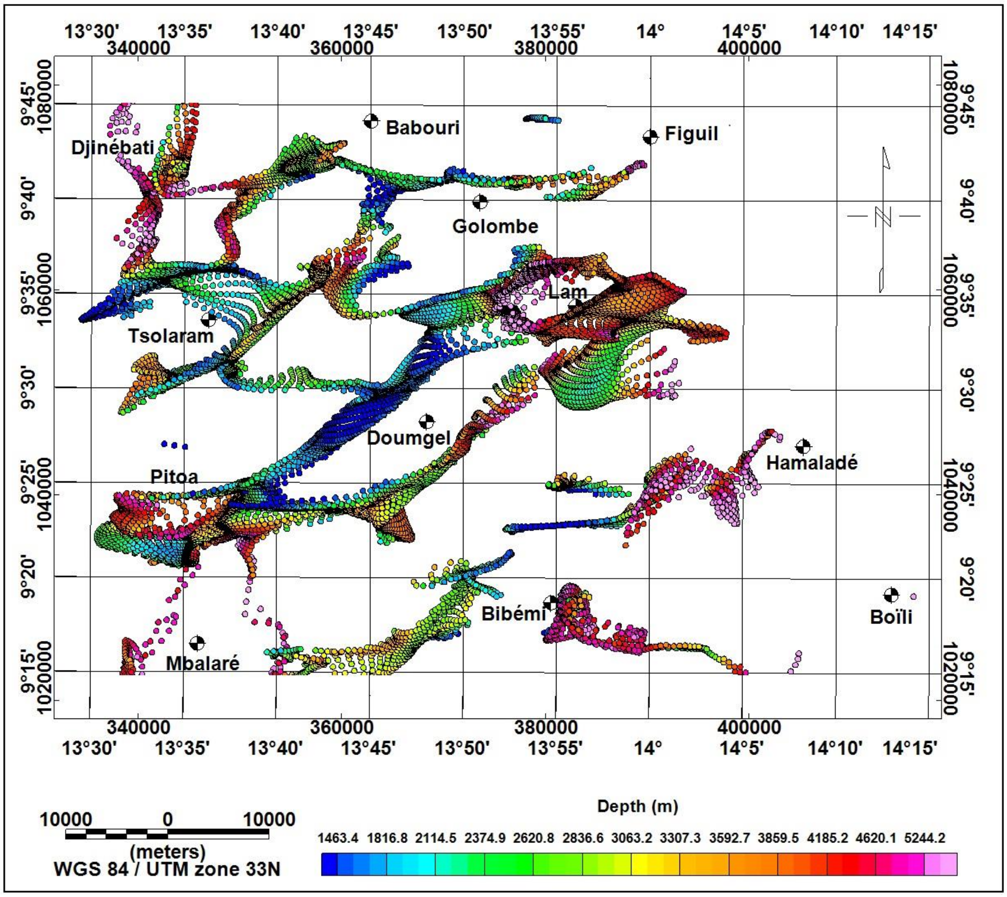

Figure 6: Euler's solutions map

Referring to the Blakely and Simpson (1986) method, the combined analysis of the Euler's solution map (Fig. 6) and the superposition of peaks map (Fig. 5) obtained from the HGM and AS maps permits us to generate the deep faults map (Fig. 7).

The faults map counts a total of 36 faults mainly directed to NW-SE, E-W and NE-SW. The Table 1 below presents the characteristics of some of these faults, namely their respective dip and depth.

https://doi.org/10.5194/se-2020-135
Preprint. Discussion started: 2 September 2020

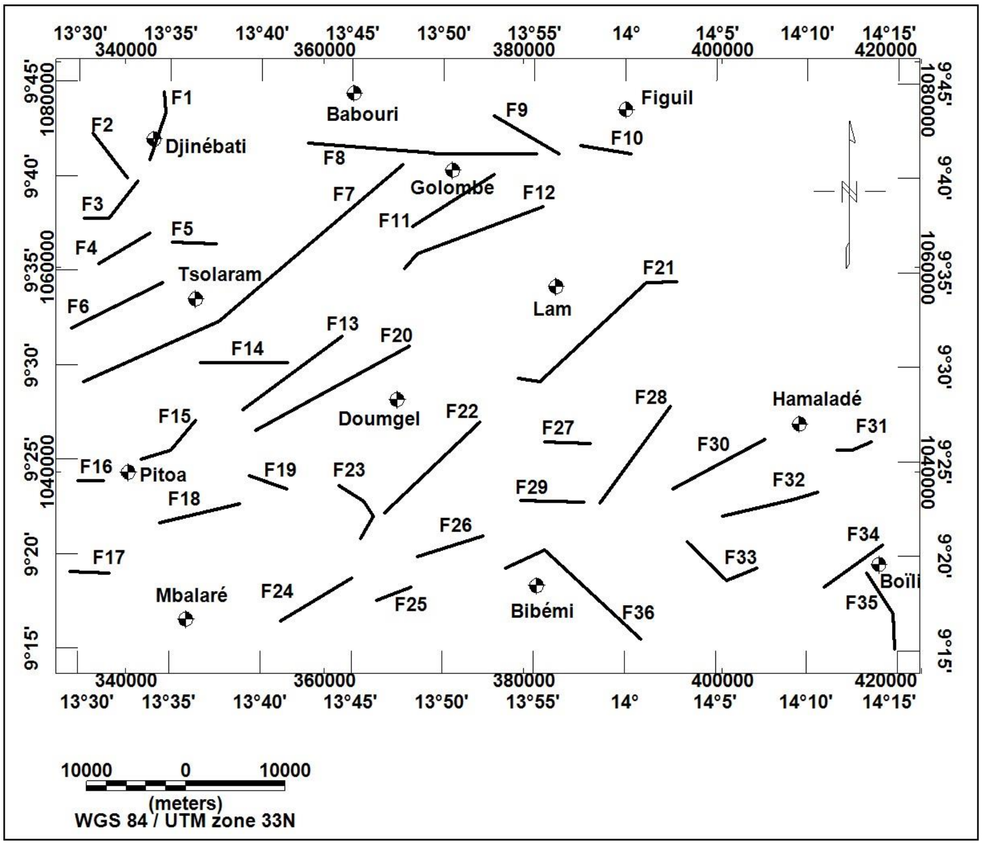

Figure 7: Faults map resulting from Euler's solutions and HGM-AS maxima maps

Dips are mainly N-W and the deepest faults are in the south of the surveyed area. The contact zone between biotite anatexite and migmatite gneisses formations is well marked by a large number of faults (F9, F12, F13, F15, F16 and F20).

Given its direction, the fault F7 could be associated to the tectonic line observed in western Golombe as it is shown in the geological map (Fig. 1).

https://doi.org/10.5194/se-2020-135
Preprint. Discussion started: 2 September 2020

Faults	Dip	Depth (m)
F1	S-E	2600
F4	N-W	1400
F5	N	2000
F6	Vertical	1400
F7	Vertical	2500
F12	N-W	1500
F13	N-W	1400
F15	N-W	1900
F19	S	3000
F21	N-W	4300
F22	N-W	2600
F23	S-W	3500
F24	N-W	3300
F26	N-W	2500
F27	N	1800
F28	N-W	4700
F29	N	1400
F30	N-W	4500

Table 1: Faults characterization of the studied area

4.5. 2.75D magnetic models

The two magnetic models (Fig. 8 and Fig. 9) are carried out respectively from profiles P1 and P2 drawn on the RTE map (Fig. 2). The earth's magnetic field, the declination, and the inclination of the region were used as main input parameters. Referring to the geological map, the profile P1 over cross from south to north: upper gneisses, monchiquite basalts of the Benue valley, rhyolitic tuffs, alluviums, Kontcha sandstone conglomerate and anatexia granites. While the profile P2 extends along the axis Djinébati-Mbalaré, over cross from the south to north: alluviums, migmatite gneisses, biotite anatexite and anatexia granites. Magnetic properties for a given model layer, are assumed continuous and constant.

https://doi.org/10.5194/se-2020-135
Preprint. Discussion started: 2 September 2020

Solid Earth
Discussions
Open Access

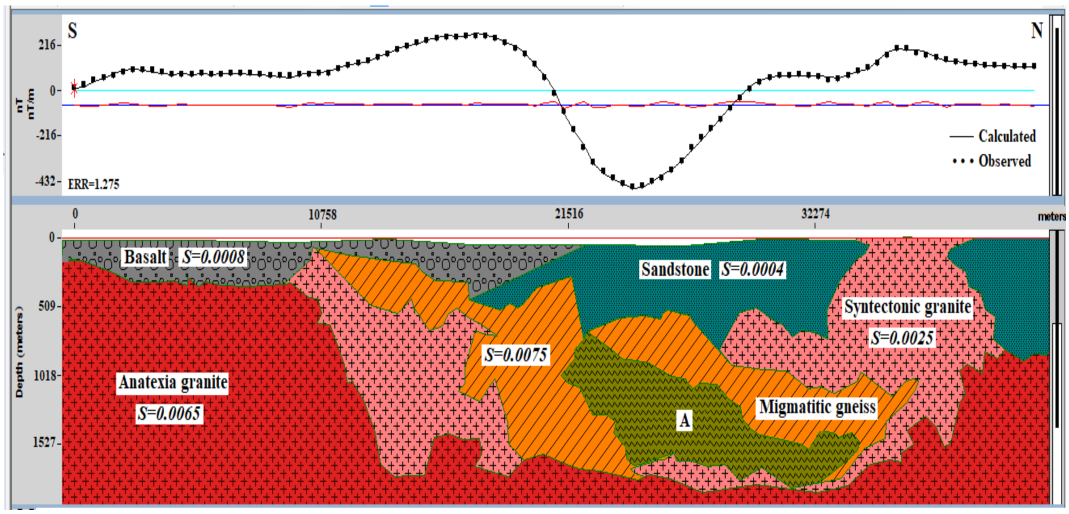

Figure 8: 2.75D model obtained from profile P1

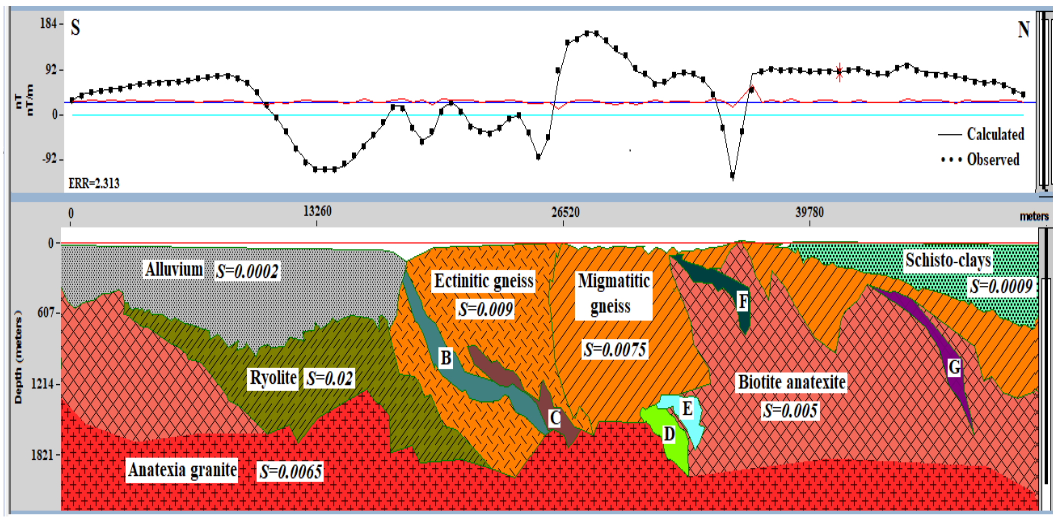

Figure 9: 2.75D model obtained from profile P2

4.5.1. Profile P1

The profile P1 is 41370.7 metres long (X). According to Skalbeck et al. (2005), the strike lengths is Y=31028.1 metres. Starting from south to north, the curve of the profile P1 passes through three major anomalies on the RTE map: the first one (positive intensity) is at the northern Bibémi, the second (negative) is in the Lam area and the third one (positive) is in the Figuil area. This justifies the fact that this curve is in the form of a potential well (U-shape).

https://doi.org/10.5194/se-2020-135
Preprint. Discussion started: 2 September 2020

Regarding the layout of formations, we have a granitic basement whereas on the surface, basalt rocks are distinctly separated from a sediments deposit, which correlates in part with the information given by the geological map (Fig. 1) since this does not reveal the presence of basalt in the northern Bibémi but rather in the Lam area. Given the lithology of the magnetic model, we can also see that the syntectonic granite formation was set up well before the migmatite gneiss formation. The previous formation is intruded by a large body A with a susceptibility value of S = 0.03 SI. Given its susceptibility (Clark and Emerson, 1991) and the environment in which it is found, the body A could be diorite because gneiss with diorite composition is listed on the geological map all around the studied area.

4.5.2. Profile P2

The profile P2 is 51867.4 metres long (X). According to Skalbeck et al. (2005), the strike lengths is Y=38900.6 metres. Starting from south to north, the curve of the profile P2 passes through several anomalies with variable wavelength from one to another alternatively positive and negative, hence a much wavy curve with several peaks. This reflects the fact that this part of the studied area has much more rugged subsurface. In other words, it has undergone many tectonic events, which could be at the origin of several infiltrations from where the plurality of intrusive bodies observed in layers.

The basement is made of granitic formation on which rests a biotite anatexite layer intruded by three bodies E, F and G with respective susceptibility value of -0.0001, 0.015 and 0.007 SI. At this layer, a formation of rhyolite is juxtaposed. On the surface we have an alluvial deposit which is separated from the schisto-clays by two gneiss formations, namely ectinite gneiss and migmatite gneiss. Ectinite gneiss is intruded by two bodies B and C with respective susceptibility value of -0.003 and -0.00001 SI.

From these magnetic models, we deduce that our studied area rests on a granitic basement which, according to the geological map, dates from the Precambrian period. The predominant rock is migmatite gneisses which is a formation directly connected to the basement in some places.

Given the environment of intrusive bodies and their susceptibility value (Clark and Emerson, 1991), a suggestion on their nature is given in Table 2.

Rock	Susceptibility	Nature
A	0.03	Diorite
B	-0.0003	Calcite
C	-0.00001	Quartz
D	0.013	Diopside
E	-0.0001	Graphite
F	0.15	Pyroxenite
G	0.007	Amphibolite

Table 2: Nature suggestion of intrusive bodies

5. Discussion

The choice of the window used for Euler's solutions is described by Marson and Klingele (1993). According to these authors, the wavelength of the observed anomalies and the grid cell define the

https://doi.org/10.5194/se-2020-135
Preprint. Discussion started: 2 September 2020

appropriate window size. Concerning the structural index (SI or N), Reid et al. (1990) concluded that low values (0 and 1) provide the best estimations of depths for sills and dykes. In this case, we focused on detection of anomaly sources, the determination of their depths and the localization of faults and contacts in the studied area, that is why we have chosen a value of N = 1. Regarding tolerance, we have set it at 15% because it is at this value that we observe a strong concordance between Euler's solutions and their depths with many short and long length wave anomalies. Concerning the Euler's solutions window, given the extent of structures in the region, we have adopted a window size of "15 kmx15 km". As we are interested by deeper structures, the last three methods above (HGM, AS and Euler Deconvolution) were applied to the upward continued RTE map to remove the outcome of superficial bodies.

From all the magnetic techniques we have applied, it transpires that dykes and faulted folds abound in the studied area. They are buried under diverse geological formations. Magnetic models show that these formations, notably gneiss and anatexite biotite, are marked by numerous intrusions.

The most of faults detected in the studied area were probably set up by the same event which affected considerably the area. This event was certainly the reactivated Pan-African shear zones.

According to Njanko et al. (2010), the NE and NW structures in the studied area result from two deformation processes recorded in the Pan-African belt, namely: senestral shearing and dextral shearing. In addition, the N-S Gode-Gormaya shear zone (GGSZ) is probably also at the origin of some highlighted faults (Ngako et al., 2008).

Faults with NE-SW dip are the most abundant. They are found in the area underlained by migmatite gneisses and biotite anatexite formations. This is in accordance with the investigations of Njandjock et al. (2006) for whom, most of faults in the studied area and surrounding areas are covered by gneiss, sand or basalt. Magnetic models indicate the presence of basalts and gneisses on the surface (Fig. 8 and 9), they are approving the thoughts of the authors above.

Furthermore, because of the same trending, the magnetic anomalies observed in the studied area could also be the consequences of the Eburnean orogeny would have intensively modified the northern Cameroon substratum. At the Cretaceous times, the setup of the Atlantic Ocean is one of the most important events that affected the geodynamic evolution of the studied area (Nguimbous et al., 2010). This event can also explain the opening of the above-mentioned faults and the very upheaval layout of formations (vertical contacts) presented by magnetic models.

6. Conclusion

The purpose of this work was to help make the knowledge about Pitoa-Figuil basement easy to understand. The combination of graphical methods (RTP) and analytical methods (HGM, AS, Euler deconvolution) highlighted contact zones of some geological formations and permitted to locate magnetic sources and estimate their depths related to shearing deformations. Results of these complementary methods helped to characterize 18 faults in the studied area. Their major dip is N-W. The location of boundary between the migmatite gneisses and biotite anatexite formations given by the geological map is confirmed. After justifying the depth values of faults described by the Euler deconvolution, magnetic models have shown that our studied area has undergone numerous

https://doi.org/10.5194/se-2020-135
Preprint. Discussion started: 2 September 2020

tectonic events (several intrusions). Most of the contacts are vertical. These models have also taught us that the basement of our studied area is granitic, above which rest certain formations that are flush with the surface. Furthermore, this study allowed us to suspect that, the settlement of the Benue tectonic trough after the opening of the Atlantic, impacted the studied area subsurface in the Northern Cameroon.

Data Availability

The data used to support the findings of this study are available from the corresponding author upon request.

Author Contribution

Voltaire Souga Kassia performed the data analyses, modelling and preliminary interpretation including preparation of the manuscript in conjunction with all the co-authors; Theophile Ndougsa-Mbarga design the topic, gives the orientations for the investigation and reviewed the quality of the models and related interpretation and the entire manuscript **;** Arsène Meying defines the criteria and the physical parameters for the 2D3/4 modelling with the first author; Jean Daniel Ngoh and Steve Ngoa Embeng have worked on the review of quality and quantitative analyses of respectively maps and 2D3/4 models.

Competing Interest

The authors declare that there are no conflicts of interest regarding the publication of this paper.

Acknowledgements

The authors are grateful to the reviewers for their valuable observations and constructive remarks making the manuscript being clearer.

References

Awoyemi, M. O., Babatunde, A. A., Sesan, C. F., Abiodun, A. E., Sakiru, O. H., Olatunbosun, A. A., and Chinwike, O. G.: Investigation of basement fault propagation in Chad Basin of Nigeria using high resolution aeromagnetic data, International Journal of Geosciences, 7, 736-744, 2016.

Blakely, R. J. and Simpson, R. W.: Approximating Edges of Source Bodies from Magnetic or Gravity Anomalies, Geophysics, 51, 1494-1498, 1986.

Clark, D. A. and Emerson, D. W.: Notes on rock magnetization characteristics in applied geophysical studies, Exploration Geophysics, 22, 547–555, 1991.

Cordell, L. and Grauch, V. J.: Mapping basement magnetization zones from aeromagnetic data in the San Juan Basin, New Mexico, 52nd Annual International Meeting, Society of Exploration Geophysicists, Dallas, 246–248, 1982.

Daouda, D.: Les plutons de Guider et de Bossoum-Pologozom (chaîne panafricaine au Nord-Cameroun) : analyses pétrographique, structurale, magnétique, géochronologique et implications géodynamiques, Ph.D. thesis, Université de Toulouse, France, 261 pp., 2014.

Durrheim, R. J. and Cooper, R. J.: EULDEP: A Program for the Euler Deconvolution of Magnetic and Gravity Data, Computers and Geosciences, 24, 6, 545-550, 1998

Feumoe, A. N., Ndougsa Mbarga, T., Manguelle Dicoum, E., and Fairhead, D.: Delineation of Tectonic Lineaments Using Aeromagnetic Data for the South-East Cameroon Area, Geofizika, 29, 175-192, 2012.

https://doi.org/10.5194/se-2020-135
Preprint. Discussion started: 2 September 2020

Solid Earth Discussions

Jeng, Y., Lee, Y. L., Chen, C. Y., and Lin, J. M.: Integrated signal enhancements in magnetic investigation in archaeology, Journal of Applied Geophysics, 53, 31–48, 2003.

Kamguia, J., Manguelle-Dicoum, E., Tabod, C. T., and Tadjou, J. M.: Geological models deduced from gravity data in the Garoua basin, Cameroon, Journal of Geophysics and Engineering, 2, 2, 147-152, 2005.

Khattach, D., Mraoui, H., Sbibih, D., and Chennouf, T. : Analyse multi-échelle par ondelettes des contacts géologiques : application à la gravimétrie du Maroc nord oriental, Geosciences, 338, 521–526, 2006.

Keating, P. and Pilkington, M.: Euler deconvolution of the analytic signal and its application to magnetic interpretation, Geophysical Prospecting, 52, 3, 165-182, 2004.

Leu, L. K.: Use of reduction to the equator process for magnetic data interpretation, Society of Exploration Geophysicists, Los Angeles, Abstract P1.2, Geophysics, 47, 445, 1981.

Marson, I. and Klingele, E. E.: Advantages of using the vertical gradient of gravity for 3D interpretation, Geophysics, 58, 1588-1595, 1993.

Ngako, V., Affaton, P., and Njongfang, E.: Pan-African Tectonics in Northwestern Cameroon, Implication for the History of Western Gondwana, Gondwana Research, 14, 509-522, 2008.

Nguimbous Kouoh, J. J., Ndougsa Mbarga, T., Njandjock Nouck, P., Eyike, A., Campos-Enriquez, J. O., and Manguelle-Dicoum, E.: The structure of the Goulfey-Tourba sedimentary basin (Chad-Cameroon): a gravity study, Geofisica Internacional, 49, 4, 412-425, 2010.

Njandjock Nouck, P., Manguelle-Dicoum, E., Ndougsa Mbarga, T., and Tabod, T. C.: Spectral analysis and gravity modelling in the Yagoua, Cameroun, sedimentary basin, Geofisica Internacional, 45, 2, 209-215, 2006.

Njanko, T., Nédélec, A., Kwékam, M., Siqueira, R., and Esteban, L.: Emplacement and Deformation of the Fomopéa Pluton: Implication for the Pan-African History of Western Cameroon, Journal of Structural Geology, 32, 306-320, 2010.

Ntsama, A. J., Bessong, M., Hell, J. V., Mbesse, C. O., Nolla, J. D., Dissombo, A. N., Edimo, Eyong, J. T., Mbassa, B. J., Mouloud, B. I., Vignaud, P. J., and Mfoumbeng, M. P.: The Importance of Diagenetic Processes in Sandstones Facies of the Hamakoussou Sedimentary Basin in North Cameroon: Influence on Reservoir Quality, International Journal of Sciences, Basic and Applied Research, 13, 2, 220-230, 2014.

Paterson, Grant, and Watson Ltd.: Études aéromagnétiques sur certaines régions de la République Unie du Cameroun. Rapport d'interprétation : Agence Canadienne de Développement International, Toronto, Canada, 1976.

Phillips, J. D.: Processing and Interpretation of Aeromagnetic Data for the Santa Cruz Basin-Patagonia Mountain Area, South Central Arizona, US Geological Survey, Open File Report, 02-98, 2001.

Rasmussen, R. and Pedersen, L. B.: End corrections in potential field modelling, Geophysical Prospecting, 27, 749–760, 1979.

Roest, W. R., Verhoef, J., and Pilkington, M.: Magnetic interpretation using the 3D analytic signal, Geophysics, 57, 116–125, 1992.

https://doi.org/10.5194/se-2020-135
Preprint. Discussion started: 2 September 2020

Solid Earth Discussions

Skalbeck, J. D., Karlin, R. E., Shevenell, L., and Widmer, M. C.: Gravity and aeromagnetic modelling of alluvial basins in the southern Truckee Meadows adjacent to the Steamboat Hills geothermal area, Washoe County, Nevada, Geophysics, 70, 3, 81-89, 2005.

Talwani, M. and Heirtzler, J. R.: Computation of magnetic anomalies caused by two-dimensional bodies of arbitrary shape, In: Parks G. A. (ed.)-Computers in the Mineral Industries, Part 1, Stanford University Publications, Geological Sciences, 9, 464–480, 1964.

Toteu, S. F., Penaye, J., and Poudjom, Y. D.: Geodynamic Evolution of the Pan-African Belt in Central Africa with Special Reference to Cameroon, Canadian Journal of Earth Sciences, 41, 73-85, 2004.

Whitehead, N. and Musselman, C.: Processing, Analysis and Visualization System for 3D Inversion of Potential Field Data in Oasis montaj v6.1. Montaj Grav/Mag Interpretation, https://fr.scribd.com/document/349623750/montajGravMagInterpretation-pdf/, last access: 11 June 2020, 2005.